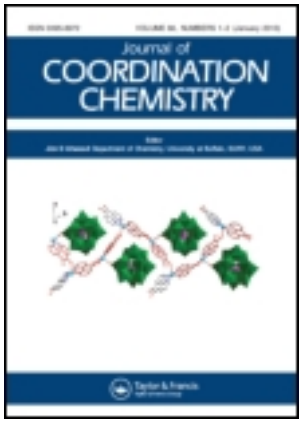

Journal of Coordination Chemistry
Publication details, including instructions for authors and subscription information:
http://www.tandfonline.com/loi/gcoo20

Carboxylate-bridged copper(II) complexes: synthesis, crystal structures, and superoxide dismutase activity

Ram N. Patel[a], Dinesh K. Patel[a], Krishna K. Shukla[a] & Yogendra Singh[a]
[a] Department of Chemistry, A.P.S. University, Rewa, India
Accepted author version posted online: 07 Nov 2013.Published online: 04 Dec 2013.

To cite this article: Ram N. Patel, Dinesh K. Patel, Krishna K. Shukla & Yogendra Singh (2013) Carboxylate-bridged copper(II) complexes: synthesis, crystal structures, and superoxide dismutase activity, Journal of Coordination Chemistry, 66:23, 4131-4143, DOI: 10.1080/00958972.2013.862790

To link to this article: http://dx.doi.org/10.1080/00958972.2013.862790

Journal of Coordination Chemistry, 2013
Vol. 66, No. 23, 4131–4143, http://dx.doi.org/10.1080/00958972.2013.862790

Carboxylate-bridged copper(II) complexes: synthesis, crystal structures, and superoxide dismutase activity

RAM N. PATEL*, DINESH K. PATEL, KRISHNA K. SHUKLA and YOGENDRA SINGH

Department of Chemistry, A.P.S. University, Rewa, India

(*Received 17 May 2013; accepted 25 October 2013*)

Two copper(II) complexes, $[Cu_2(\mu\text{-benzoato})(L^1)_2]NO_3{\cdot}2H_2O$ (**1**) and $[Cu_2(\mu\text{-succinato})(L^2)_2(H_2O)]ClO_4$ (**2**), have been synthesized, where L^1 = N′-[(E)-phenyl(pyridin-2-yl)methylidene]benzoylhydrazone and L^2 = N′-[(E)-pyridin-*2*-ylmethylidene]benzoylhydrazone. These complexes were characterized including by single-crystal X-ray diffraction studies. The copper is five-coordinate in **1** while in **2** one copper is five-coordinate and the other is six-coordinate. Electrochemical behavior of these complexes was measured by cyclic voltammetry. The conproportionation equilibrium constants (K_{con}) for both complexes have been estimated. The superoxide dismutase (SOD) activities of **1** and **2** were measured by nitro blue tetrazolium assay. Complex **1** has better SOD activity than **2**.

Keywords: Carboxylate-bridged copper(II); Crystal structure; EPR spectra; SOD activity

1. Introduction

Dinuclear copper complexes have received attention as model compounds for the active site of biological copper enzymes [1–10]. Copper(II) carboxylate complexes form an interesting class of compounds in that they are relatively easily prepared with a high degree of purity. They form both monomeric and dimeric complexes and in some cases show an unusual temperature dependence in their ESR spectra [11] and a large variation in the singlet–triplet separation energies [12–14]. Interest in carboxylate copper(II) complexes, besides from the point view of pure coordination chemistry, has led to investigations of their pharmacological properties, antiradical and antiphlogistic activities. The proposed curative properties of copper-based non-steroidal anti-inflammatory drugs have led to development of a group of copper(II) complexes with enhanced antiphlogistic activity compared with their uncomplexed parent compounds [15–17]. This biological activity was also observed in a group of mononuclear and binuclear carboxylate-bridged copper(II) complexes and even in copper(II) complexes with Schiff bases of N-salicylideneaminoalkanoate type [18, 19]. According to the above mentioned findings, low-molecular weight carboxylate-bridged copper(II) complexes can be beneficial in affecting inflammation processes. Several interesting

*Corresponding author. Email: rnp64@ymail.com

complexes have been reported [20–23] using benzoic acid, naphthyl acetic acid, sebacic acid, 2,5-dibenzoyl terephthalic acid, and diester carboxylic acids. This work is an extension of our recent reports in understanding the structural, electrochemical, and biological properties of copper(II) binuclear systems [24].

2. Experimental

2.1. *Materials*

Copper(II) nitrate trihydrate was purchased from S.D. fine chemicals, India. All other chemicals were of synthetic grade and used without purification.

2.2. *Physical measurements*

2.2.1. Elemental analysis. Elemental analyzes of the complexes were performed on an Elemental Vario EL III Carlo Erba 1108 analyzer. FAB mass spectra were recorded on a JEOL SX 102/DA 6000 mass spectrometer/data system using xenon (6 kV, 10 mA) as the FAB gas. The accelerating voltage was 10 kV and spectra were recorded at room temperature (RT).

2.2.2. Spectroscopy. UV–vis spectra were recorded at 25 °C on a Shimadzu UV–vis recording spectrophotometer UV-1601 in quartz cells. Infrared (IR) spectra were recorded in KBr on a Perkin-Elmer 783 spectrophotometer. X-band electron paramagnetic resonance (EPR) spectra were recorded with a Varian E-line Century Series Spectrometer equipped with a dual cavity and operating at X-band with 100 kHz modulation frequency. Varian quartz tubes were used for measuring EPR spectra of polycrystalline samples and frozen solutions. Tetracyanoethylene was used as marker ($g_{\|}$ = 2.00277). The EPR parameters for copper(II) complexes were determined accurately from a computer simulation program [25–27].

2.2.3. Magnetic susceptibility. Magnetic susceptibility measurements were made on a Gouy balance using mercury(II) tetrathiocyanato cobaltate(II) as calibrating agent ($\chi_g = 16.44 \times 10^{-6}$ c.g.s. units).

2.2.4. Electrochemistry. Cyclic voltammetry (CV) was carried out with a BAS-100 Epsilon Electrochemical Analyzer having an electrochemical cell with a three-electrode system. Ag/AgCl was used as reference electrode, glassy carbon as working electrode, and platinum wire as an auxiliary electrode; 0.1 M L^{-1} $NaClO_4$ was used as supporting electrolyte and DMSO as solvent. All measurements were carried out at 298 K under nitrogen.

2.2.5. Superoxide dismutase (SOD) activity. The *in vitro* SOD activity was measured using alkaline DMSO as a source of superoxide radical (O_2^-) and nitro blue tetrazolium (NBT) chloride as O_2^- scavenger [28]. In general, 400 mL sample to be assayed was added

to a solution containing 2.1 mL of 0.2 M L^{-1} potassium phosphate buffer (pH 8.6) and 1 mL of 56 mM L^{-1} alkaline DMSO solution was added while stirring. The absorbance was then monitored at 540 nm against a sample prepared under similar condition except NaOH was absent. A unit of SOD activity is the concentration of complex, which causes 50% inhibition of alkaline DMSO-mediated reduction of NBT.

2.3. *Synthesis*

2.3.1. Synthesis of L^1. The Schiff base L^1 was synthesized by condensation of benzoylpyridine and benzoylhydrazide in 1 : 1 ratio. The reaction mixture in ethanol was stirred for 4 h until a colorless solution was obtained, filtered, and left for slow evaporation at RT. White block-shaped crystals were collected by filtration and washed with diethyl ether. Anal. Calcd $C_{19}H_{15}N_3O$: C, 75.73; H, 5.02; N, 13.94%. Found: C, 75.50; H, 4.98; N, 14.02%. FAB mass (m/z) Calcd 301.34; Found: 301.

2.3.2. Synthesis of L^2. The Schiff base L^2 was prepared by condensation of pyridinecarboxaldehyde and benzoylhydrazine. A solution of 2-pyridinecarboxaldehyde (1.071 g, 10.0 mM) in 10 mL ethanol was refluxed with an ethanolic solution of benzoylhydrazine (1.361 g, 10.0 mM) continuously for 6 h. After some time 1–2 drops of acetic acid was added. On cooling the solution at RT, pale yellow crystals separated, were filtered off, and washed with methanol. These were dried in air at RT and stored in a $CaCl_2$ desiccator. Anal. Calcd for $C_{13}H_{11}N_{30}$: C, 69.32; H, 4.92; N, 18.66%. Found: C, 69.02; H, 4.56; N, 18.45%.

2.3.3. Synthesis of $[Cu_2(\mu\text{-benzoato})(L^1)_2]NO_3{\cdot}2H_2O$ (1). Complex **1** was synthesized by reaction of copper(II) nitrate (1 mM, 0.241 g) with benzoic acid (0.5 mM, 0.061 g) and L_1 (1 mM, 0.301 g) in methanol (20 mL). The resulting mixture was stirred for 2 h and after slow vaporization at RT light blue crystals suitable for single crystal study were obtained. Crystals were dried in air at RT and stored in a $CaCl_2$ desiccator. Anal. Calcd for $C_{45}H_{33}Cu_2N_7O_9$: C, 57.32; H, 3.52; N, 10.40%. Found: C, 57.02; H, 3.56; N, 10.45%.

2.3.4. Synthesis of $[Cu_2(\mu\text{-succinato})(L^2)_2(H_2O)]ClO_4$ (2). Complex **2** was synthesized by dissolving copper(II) perchlorate (1 mM, 0.370 g) with succcinic acid (0.5 mM, 0.09 g) and L_2 (1 mM, 0.225 g) in methanol (20 mL). The resulting mixture was stirred for 4 h. After slow vaporization at RT light blue crystals suitable for single crystal study were obtained. Crystals were dried in air at RT and stored in a $CaCl_2$ desiccator. Anal. Calcd for $C_{30}H_{25}ClCu_2N_6O_{11}$: C, 44.59; H, 3.12; N, 10.40%. Found: C, 45.02; H, 3.16; N, 10.45%.

2.3.5. Single-crystal X-ray crystallography. Single-crystal X-ray data were collected on a CCD detector based Oxford Diffractometer using graphite-monochromated Mo-Kα (λ = 0.71073 Å) radiation. The diffraction data were solved using SIR-92 [29] with GUI control and the structures were refined by SHELXL-97 [30] refinement of F^2 against all reflections. Non-hydrogen atoms were refined anisotropically and all hydrogens were geometrically fixed and allowed to refine using a riding model. The hydrogens of water

were taken from difference Fourier maps and were independently refined. Molecular graphics were generated using ORTEP-3v2 for WINDOWS [31], PLATON [32], and Mercury [33].

2.3.6. SOD activity. The SOD activities of the present copper(II) complexes were evaluated using alkaline DMSO as the superoxide radicals (O_2^-) generating system in association with NBT chloride as a scavenger of superoxide [34, 35]. In certain concentration of the complex solution, 2.1 mL of 0.2 M potassium phosphate buffer (8.6 pH) and 1 mL of 56 μM NBT solutions were added. The mixture was kept in ice for 15 min and then 1.5 mL of alkaline DMSO solution was added while stirring. The reduction of NBT was monitored at 540 nm on a Shimadzu UV-1601 spectrophotometer against a sample prepared under similar condition except NaOH was absent in DMSO. The SOD activities of the complexes were evaluated by the 50% inhibitory concentration (IC_{50}) and compared with the native Cu-Zn SOD enzyme.

3. Results and discussion

3.1. *Synthesis*

Copper(II) complexes were prepared by reaction of metal salt with hydrazone Schiff base. Conventional solution method was adopted for synthesis and crystalline products suitable for single-crystal X-ray diffraction studies have been obtained. The target complexes were first characterized by elemental analysis. Suitable crystals were selected for single-crystal X-ray analysis. Both complexes are binuclear.

3.2. *Crystallographic study of $[Cu_2(\mu\text{-benzoato})(L^1)2]NO_3{\cdot}2H_2O$ (1)*

An ORTEP presentation of the structure of $[Cu_2(\mu\text{-benzoato})(L^1)_2]NO_3{\cdot}2H_2O$ (**1**) with atom-numbering scheme is shown in figure 1 and crystal data and structure refinement data for both complexes are given in table 1. The copper(II) centers of **1** are coordinated by two nitrogens and one oxygen of tridentate hydrazone and one oxygen of benzoate. Hydrazone ligand is present as the enolic form instead of keto form and enolic oxygen bridges two copper(II) centers along with benzoate. The coordination environment around the copper(II) is five-coordinate. The trigonality index τ is calculated using the equation $\tau = (\beta\text{-}\alpha)/60$ [36] (for perfect square pyramidal and trigonal bipyramidal geometries the values of τ are zero and unity, respectively). The value of τ for Cu(1) is 0.123 and for Cu(2) is 0.204, indicating distorted square pyramidal geometry. Selected bond lengths and angles for **1** are given in table 2. The μ-benzoato bridges two distorted square pyramidal copper(II) ions in *syn*, *syn*-η 1 : η 1 : μ having a Cu···Cu distance of 3.1032(10) Å.

3.3. *Crystallographic study of $[Cu_2(\mu\text{-succinato})(L^2)_2(H_2O)]ClO_4$ (2)*

The ORTEP structure of **2** is displayed in figure 2 and a selection of pertinent crystallographic data are presented in table 1. Selected bond lengths and angles are listed in table 3. Complex **2** also has an enolic bridge like **1** along with a succinate bridge. The

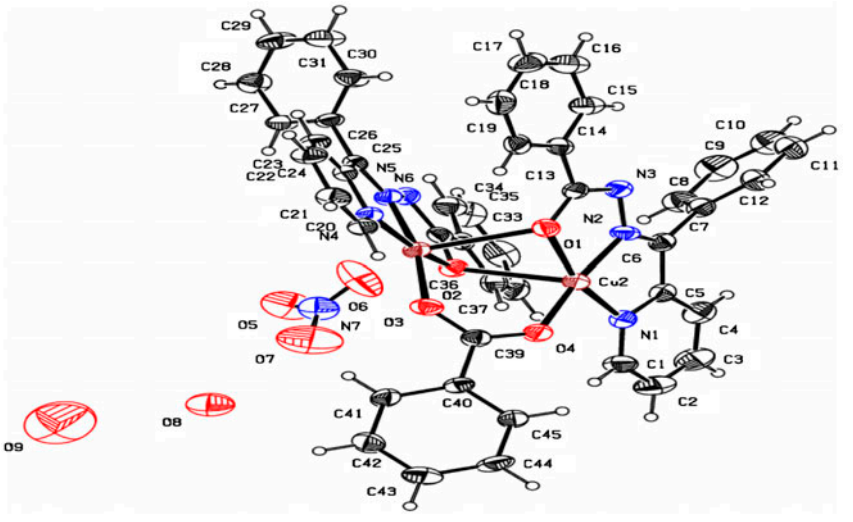

Figure 1. ORTEP structure of $[Cu_2(\mu\text{-benzoato})(L^1)_2]NO_3{\cdot}2H_2O$ (**1**).

copper(II) centers have different coordination geometry. Cu(1) is six-coordinate while Cu(2) is five-coordinate. The square pyramidal geometry of Cu(2) was confirmed and quantified by the analysis of τ parameter. The value of τ for Cu(2) is 0.245, indicating some distortion from the ideal square pyramidal geometry. One succinate bridges two copper(II) ions in *syn*, *syn*-η 1 : η 1 : μ having a Cu···Cu distance of 3.1716(12) Å. The crystal structure of **2** contains two perchlorates which are involved in additional stability.

3.4. *Electronic and IR spectra*

Electronic spectra of both complexes were recorded in 100% DMSO solution. The spectra of **1** and **2** show a fairly broad band at ~680 nm. In addition, LMCT transition at ~395 nm is sensitive for the bridged Cu–Cu system [37]. The latter band is also present in the diffuse reflectance spectrum of the complexes together with a broad d–d band at 715 nm. The d–d band for both complexes shifted going from solid to solution, attributed to the different constraints imposed to the copper coordination site by the solid state and coordination of solvent. The IR spectra of **1** and **2** were recorded from 4000 to 400 cm^{-1}. The spectra show characteristic absorptions at 1680, 1575, and 1080 cm^{-1} due to ν(C=O), ν(C=N), and ν(N–N), respectively. The band at 3140 cm^{-1} is absent in the complexes, indicating that ligand is present in the enolic form. The formation of enolic form in the complexes is confirmed by two new bands at 1590–1490 cm^{-1} and 1360–1380 cm^{-1} that are assigned to ν(C=N–N=C) and ν(C–O), respectively [38]. In IR spectra of **1**, the strong absorption at 1360 cm^{-1} indicates the presence of nitrate [39]. Similarly, absorptions at 1105, 1140, and 1185 cm^{-1} of **2** are due to uncoordinated perchlorate [40].

Table 1. Crystal data and structure refinement parameters for **1** and **2**.

Empirical formula	$C_{45}H_{33}Cu_2N_7O_9$ Benzoic acid	$C_{30}H_{25}ClCu_2N_6O_{11}$ Succinic acid
Formula weight	942.86	808.11
Temperature (K)	293(2)	153(2)
Wavelength (Å)	0.71073	0.71073
Crystal system	Triclinic	Triclinic
Space group	*P-1*	*P-1*
Unit cell dimensions		
a (Å)	12.2388(11)	9.911(2)
b (Å)	12.7385(7)	12.556(3)
c (Å)	14.7418(13)	15.579(3)
α (°)	73.414(7)	98.46(3)
β (°)	75.183(8)	108.40(3)
γ (°)	84.723(6)	106.39(3)
Volume ($Å^3$)	2129.0(3)	1704.4(6)
Z	2	2
Calculated density	1.471	1.575
Absorption coefficient	1.064	1.393
F(000)	964	820
Crystal size	0.28 × 0.24 × 0.20	0.36 × 0.23 × 0.08
θ Range for data collection	2.99–24.18	1.43–25.00
Limiting indices	$-14 <= h <= 8$, $-14 <= k <= 14$, $-16 <= l <= 16$	$-11 <= h <= 11$, $-14 <= k <= 14$, $18 <= l <= 18$
Reflections collected/ unique	15,506/6724 [*R*(int) = 0.0452]	16,397/5986 [*R*(int) = 0.0276]
Completeness to $\theta = 25.00°$	98.6%	99.7%
Absorption correction	Semi-empirical from equivalents	None
Max. and min. transmission	0.808 and 0.750	–
Refinement method	Full-matrix least-squares on F^2	Full-matrix least-squares on F^2
Data/restraints/parameters	6724/2/568	5986/2/459
Goodness-of-fit on F^2	0.857	1.048
Final *R* indices [$I > 2\sigma(I)$]	*R*1 = 0.0468, w*R*2 = 0.1004	*R*1 = 0.0631, w*R*2 = 0.2004
R indices (all data)	*R*1 = 0.0940, w*R*2 = 0.1091	*R*1 = 0.0744, w*R*2 = 0.2129
Largest diff. peak and hole (e $Å^{-3}$)	0.698 and −0.513	1.632 and −0.831

Table 2. Selected bond lengths (Å) and angles (°) for **1**.

Bond lengths			
Cu(1)–O(3)	1.891(4)	Cu(2)–N(2)	1.891(4)
Cu(1)–N(5)	1.907(4)	Cu(2)–O(4)	1.903(4)
Cu(1)–O(2)	1.970(4)	Cu(2)–O(1)	1.971(3)
Cu(1)–N(4)	1.973(4)	Cu(2)–N(1)	1.999(5)
Bond angles			
O(3)–Cu(1)–N(5)	169.18(17	C(13)–O(1)–Cu(2)	109.1(3)
O(3)–Cu(1)–O(2)	100.85(15)	C(39)–O(3)–Cu(1)	128.4(4)
N(5)–Cu(1)–O(2)	80.34(17)	C(32)–O(2)–Cu(1)	109.8(3)
O(3)–Cu(1)–N(4)	97.09(17)	C(20)–N(4)–Cu(1)	128.1(4)
N(5)–Cu(1)–N(4)	81.26(19)	C(24)–N(4)–Cu(1)	113.1(4)
O(2)–Cu(1)–N(4)	161.59(17)	C(39)–O(4)–Cu(2)	130.4(4)
N(2)–Cu(2)–O(4)	173.59(19)	C(25)–N(5)–Cu(1)	119.6(4)
N(2)–Cu(2)–O(1)	79.67(18)	N(6)–N(5)–Cu(1)	117.2(3)
O(4)–Cu(2)–O(1)	103.15(16)	C(1)–N(1)–Cu(2)	128.9(4)
N(2)–Cu(2)–N(1)	81.7(2)	C(5)–N(1)–Cu(2)	112.4(4)
O(4)–Cu(2)–N(1)	95.45(19)	C(6)–N(2)–Cu(2)	119.5(4)
O(1)–Cu(2)–N(1)	161.34(18)	N(3)–N(2)–Cu(2)	119.5(4)

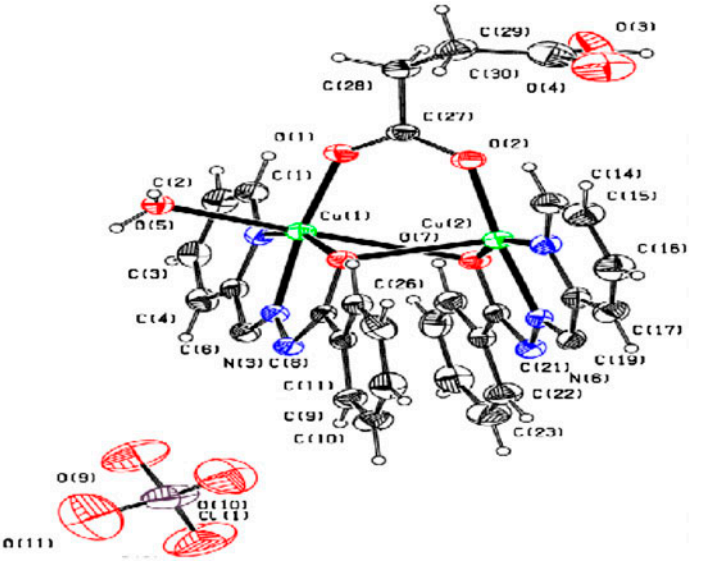

Figure 2. ORTEP structure of $[Cu_2(\mu\text{-succinato})(L^2)_2(H_2O)]ClO_4$ (**2**).

Table 3. Selected bond lengths (Å) and angles (°) for **2**.

Bond lengths			
N(1)–Cu(1)	2.008(4)	N(2)–Cu(1)	1.936(4)
N(2)–N(3)	1.367(5)	N(4)–Cu(2)	2.009(5)
N(5)–N(6)	1.366(6)	N(5)–Cu(2)	1.918(4)
O(1)–Cu(1)	1.933(4)	O(2)–Cu(2)	1.917(4)
O(5)–Cu(1)	2.304(4)	O(7)–Cu(2)	1.968(4)
O(6)–Cu(1)	1.984(3)	O(6)–Cu(2)	2.391(3)
O(3)–H(3A)	0.8200		
Bond angles			
C(18)–N(4)–Cu(2)	111.8(4)	C(1)–N(1)–Cu(1)	129.3(4)
C(14)–N(4)–Cu(2)	128.7(4)	C(5)–N(1)–Cu(1)	112.5(3)
C(19)–N(5)–N(6)	123.7(4)	C(6)–N(2)–Cu(1)	117.8(3)
C(19)–N(5)–Cu(2)	118.2(4)	N(3)–N(2)–Cu(1)	117.5(3)
C(19)–N(5)–N(6)	123.7(4)	C(27)–O(2)–Cu(2)	131.5(4)
C(27)–O(1)–Cu(1)	128.4(3)	C(7)–O(6)–Cu(1)	110.9(3)
C(7)–O(6)–Cu(2)	114.8(3)	C(20)–O(7)–Cu(2)	109.9(3)
Cu(1)–O(6)–Cu(2)	92.48(13)	O(1)–Cu(1)–N(2)	173.37(16)
N(2)–Cu(1)–O(6)	78.67(16)	O(1)–Cu(1)–O(6)	99.84(15)
O(1)–Cu(1)–N(1)	100.19(17)	N(2)–Cu(1)–N(1)	80.59(18)
O(6)–Cu(1)–N(1)	158.68(17)	O(2)–Cu(2)–N(5)	174.70(17)
O(1)–Cu(1)–O(5)	90.14(16)	O(2)–Cu(2)–O(7)	102.15(16)
N(2)–Cu(1)–O(5)	96.43(16)	N(5)–Cu(2)–O(7)	79.49(17)
O(6)–Cu(1)–O(5)	95.59(15)	O(2)–Cu(2)–N(4)	96.99(18)
N(1)–Cu(1)–O(5)	91.59(17)	N(5)–Cu(2)–N(4)	80.92(19)
O(7)–Cu(2)–N(4)	159.95(17)	O(2)–Cu(2)–O(6)	88.35(15)
N(5)–Cu(2)–O(6)	96.74(15)	O(7)–Cu(2)–O(6)	89.22(14)
N(4)–Cu(2)–O(6)	97.29(16)		

3.5. *Electrochemistry*

The electrochemical properties of **1** and **2** have been studied by CV under nitrogen in DMSO solution from +1.2 V to −1.2 V *versus* Ag/AgCl reference electrode. The electrochemical properties have been studied to monitor spectral and structural changes accompanying electron transfer [41]. A representative cyclic voltammogram is shown in figure 3. Two-one electron reduction responses are observed presumably due to the following electrode reactions:

$$Cu^{II} - Cu^{II} + e^- \rightarrow Cu^{II} - Cu^{I}$$

$$Cu^{II} - Cu^{I} + e^- \rightarrow Cu^{I} - Cu^{I}$$

These indicate significant metal coupling in both complexes [42–44]. These redox couples are quasireversible with an average peak separation between the cathodic and anodic waves of 0.15 V. CV data along with conproportionation equilibrium constant (K_{con}) of **1** and **2** are given in table 4. The larger K_{con} is, the greater the electronic coupling. K_{con} for the equilibrium $Cu^{II}Cu^{II} + Cu^{I}Cu^{I} \rightleftharpoons 2Cu^{II}Cu^{I}$ is usually estimated from the difference in the half-wave potential between metal center couples, $\log K_{con} = 16.9(\Delta E_{1/2})$ [45]. The large K_{con} indicate that the addition of a second electron is more difficult than the first electron and the Cu^{II} Cu^{I} mixed valence complex is stable with respect to conproportionation. This observation is observed in several binuclear metal complexes [46, 47].

3.6. *Magnetic studies*

Magnetic measurements of the complexes were done at 278 K on a Gouy Balance. The effective magnetic moment (μ_{eff}) of $[Cu_2(\mu\text{-benzoato})(L^1)2]NO_3{\cdot}2H_2O$ (**1**) and $[Cu_2(\mu\text{-succinato})(L^2)_2(H_2O)]ClO_4$ (**2**) was measured to be 1.69 and 1.73 B.M, respectively. The

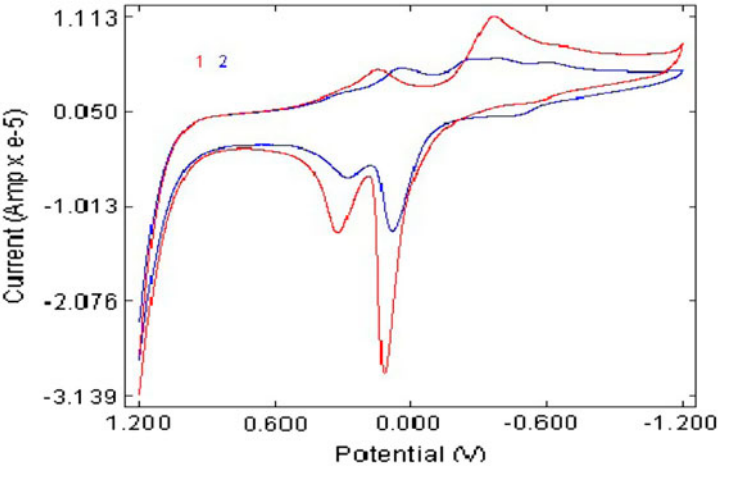

Figure 3. Cyclic voltammogram of $[Cu_2(\mu\text{-benzoato})(L^1)_2]NO_3{\cdot}2H_2O$ (**1**) and $[Cu_2(\mu\text{-succinato})(L^2)_2(H_2O)]ClO_4$ (**2**) in DMSO (0.1 M $NaClO_4$ as supporting electrolyte; scan rate: 100 mV/s).

Table 4. CV parameters for **1** and **2**.

Complex	E_{Pc1} (V)	E_{Pa1} (V)	E_{Pc2} (V)	E_{pa2} (V)	$E^1{}_{½}$ (V)	$E^2{}_{½}$ (V)	k_{con}
1	0.146	0.320	−0.367	0.117	0.087	−0.125	3.91×10^5
2	0.041	0.279	−0.269	0.083	0.119	−0.093	3.91×10^5

magnetic moment (μ_{eff}) for both complexes at RT is below the theoretical value expected for a copper(II) center with $S = ½$ and indicative of antiferromagnetic couple between the copper(II) ions through bridging units in the polycrystalline state [48]. The antiferromagnetic behavior of the binuclear complexes is attributed to spin–spin interaction via the super-exchange pathway provided by bridging groups rather than a direct metal–metal interaction [49]. The copper–copper distances in **1** and **2** are 3.10 and 3.17 Å, respectively, from X-ray diffraction studies.

3.7. *EPR studies*

EPR spectra of powdered sample of **1** and **2** were measured at RT and in frozen solution at 77 K. The spectra are shown in figures 4 and 5. For spin-coupled copper(II) systems both $\Delta M_s = \pm 1$ and $\Delta M_s = \pm 2$ transitions are predicted [41]. The $\Delta M_s = \pm 1$ transitions around $g \approx 2$ line widths depends on the distance (r) between the two copper(II) centers. At very short value of r, the EPR signal broadens and can be silent if the antiferromagnetic coupling is strong enough. In the complexes r [3.1032(10) for **1** and 3.1716(12) for **2**] was calculated from single-crystal X-ray studies. At these distances broad spectrum is usually observed and very low temperature is needed to detect a well-resolved signal. The solution EPR spectrum of **1** is axially symmetric ($g_{\parallel} = 2.249$ and $g_{\perp} = 2.062$) having a quartet hyperfine structure on the parallel component arising from the interaction of an unpaired electron.

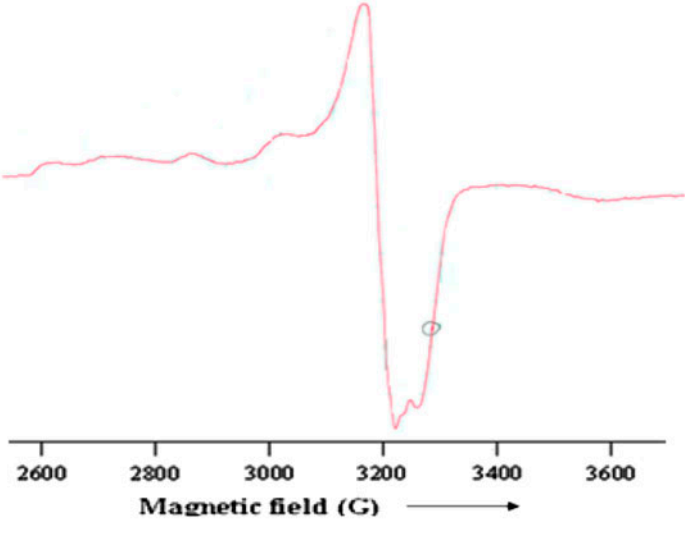

Figure 4. EPR spectrum of $[Cu_2(\mu\text{-benzoato})(L^1)_2]NO_3{\cdot}2H_2O$ (**1**) at LNT (0.003 M^{-1} dm^{-3}) in DMSO.

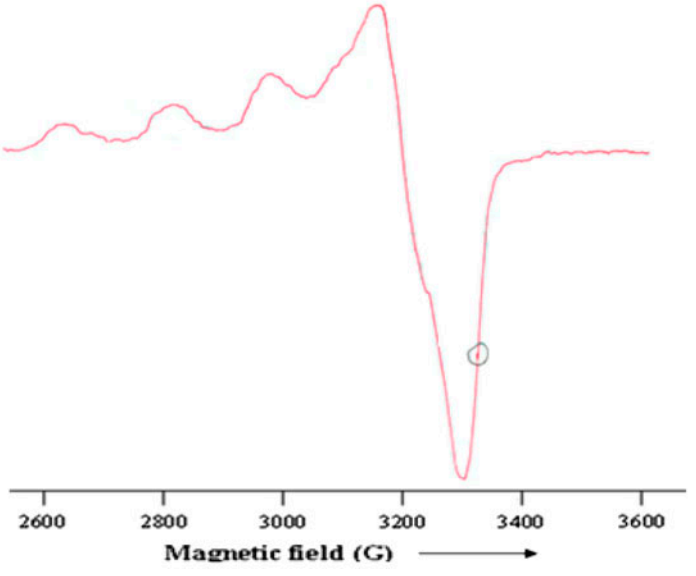

Figure 5. EPR spectrum of $[Cu_2(\mu\text{-succinato})(L^2)_2(H_2O)]ClO_4$ (**2**) at LNT (0.003 M^{-1} dm^{-3}) in DMSO.

The $g_{\parallel}$ values (table 5) are nearly the same for both complexes, indicating the bonding is dominated by the ligand.

The $g_{\parallel} > g_{\perp}$ account to the distorted square pyramidal structure of **1** and rules out the possibility of a trigonal bipyramidal structure which would be expected to have $g_{\perp} > g_{\parallel}$ [50, 51]. The EPR spectra of frozen solution of **2** at 77 K show a broad signal centered on $g_{\parallel} = 2.239$. This EPR spectral behavior agrees with the triplet signal detected in solution. In the $\Delta M_s = \pm 1$ region, four in the $g_{\parallel}$ region were observed. However, complex exhibits the usual pattern for mononuclear copper(II) complexes and showed two signals due to the presence of two different copper(II) coordination environments with parallel magnetic parameters of $g_{\parallel}$ and $A_{\parallel}$.

Table 5. EPR and UV spectral parameters of the copper(II) complexes.

Parameter		**1**	**2**
Polycrystalline state (298 K)	g_1	2.095	2.171
	g_2	2.015	2.095
DMSO (77 K)	$g_{\parallel}$	2.249	2.239
	$g_{\perp}$	2.062	2.070
	$A_{\parallel}$ (G)	202	157
	G	4.153	3.511
	α^2	0.868	0.692
	β^2	0.989	0.735
	γ^2	0.668	0.837
	$K_{\parallel}$	0.859	0.844
	$K_{\perp}$	0.850	0.872
	λ_{max} (cm^{-1})	14,662	14,285

3.8. *SOD activity*

SOD provides an important defense against toxicity of dioxygen. SOD has ability to inhibit reduction of NBT chloride. Complexes **1** and **2** exhibit catalytic activity toward the dismutation of superoxide anion. The SOD graphs of **1** and **2** are presented in figure 6. Superoxide was supplied from alkaline DMSO and SOD activity was evaluated by NBT assay [52], following kinetically the reduction of NBT at 560 nm. The concentration causing 50% inhibition of NBT reduction is called IC_{50}. The determined IC_{50} values are 38 ± 5 μM for **1** and 44 ± 5 μM for **2**. The IC_{50} values of **1** and **2** are higher than the value of native bovine erythrocyte SOD (0.04 μM), but on the same order of magnitude as the SOD analogs described in the literature [53]. The geometry around the copper site in natural Cu, Zn SOD [54] is rather distorted tetrahedral with a vacant site for binding of superoxide, with the vacant site transiently occupied by labile H_2O in the crystal structure [55]. Therefore, the distorted structure around the copper center is quite important for SOD activity. Designing ligand having a flexible backbone capable to accommodate copper ion in different geometries or alternatively ligands having limited flexibility but importing a tetrahedral like constraint is an important task. The tetrahedral distortion exerted by ligand to copper(II) in both complexes is of particular importance because it can allow easier reduction of SOD activity of copper(II) [28]. Although the SOD data of both complexes are similar, **1** is more SOD active than **2**, due to different bridging moiety and geometry of Cu(II). Similar results have been reported [28] (table 6). Such behavior is consistent with previous reports of the investigation of the use of homo dinuclear metal complexes [28, 44]. Although metal–metal interaction, as is clear from the results of the above ESR studies, is not observed in the present complexes, the geometries around Cu(II) were a mixture of five-coordinate trigonal

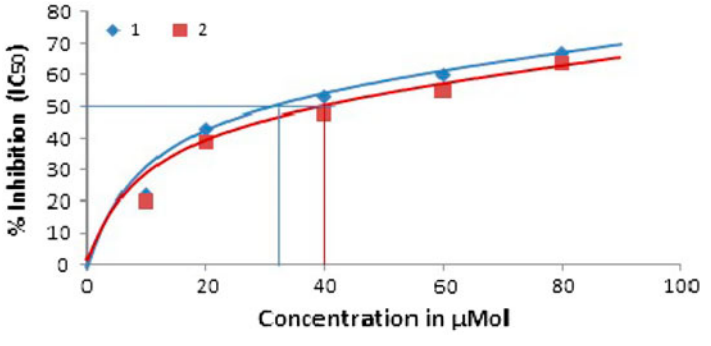

Figure 6. Graphical representation of SOD activity of **1** and **2**.

Table 6. SOD activity of some copper(II) complexes.

S.no.	Complexes	IC_{50} (μM dm^{-3})	Refs.
1.	$[(L^1)Cu\text{-}(\mu\text{-}CH_3COO)_2Cu(L^1)]$ 4,4-bipy	52	[44]
2.	$[(L^2)Cu\text{-}(\mu\text{-}NO_3)_2Cu(L^2)]$	58	[44]
3.	$[(L)Cu(\mu\text{-}CH_3COO)_2Cu(L)]$	35	[28]
4.	$[(L)Cu(\mu\text{-}NO_3)_2Cu(L)]$	26	[28]
5.	$[Cu_2(\mu\text{-benzoato})(L^1)_2]NO_3\cdot 2H_2O$	38	Present work
6.	$[Cu_2(\mu\text{-succinato})(L^2)_2(H_2O)]ClO_4$	44	Present work

bipyramidal and square pyramidal. The above findings indicate that flexibility in the copper-coordinated geometries and dinuclear center could accelerate the catalytic cycle, and the dual multidentate ligand can function both for dioxygen binding and electron transfer sites in this cycle.

4. Conclusion

We have synthesized and structurally characterized two new carboxylate-bridged copper(II) complexes (**1** and **2**). In **1,** both copper centers have distorted square pyramidal geometry while for **2** one copper has distorted square pyramidal and the other has distorted octahedral geometry. Schiff base ligand shows keto-enol tautomerism in the complexes. In both complexes, $g_{\perp} > g_{\parallel} > 2.0023$ substantiates the existence of unpaired electron in $d_{x^2-y^2}$ orbital. Both complexes showed SOD activity with **1** showing more SOD activity than **2**.

Supplemental material

CCDC 903805 and 903806 contain the supplementary crystallographic data for $[Cu_2(\mu\text{-benzoato})(L^1)_2]NO_3{\cdot}2H_2O$ (**1**) and $[Cu_2(\mu\text{-succinato})(L^2)_2(H_2O)]ClO_4$ (**2**). These data can be obtained free of charge via http://www.ccdc.cam.ac.uk/conts/retrieving.html or from the Cambridge Crystallographic Data Center, 12 Union Road, Cambridge, CB2, 1EZ, UK; Fax: (+44) 1223-336-033; or E-mail: deposit@ccdc.cam.ac.uk.

Acknowledgements

Our grateful thanks to School of Chemistry, University of Hyderabad, Hyderabad for Single Crystal X-ray data collection, RSIC (SAIF) IIT, Bombay for EPR measurements and SAIF, Central Drug Research Institute, Lucknow for providing elemental and IR spectral analysis. Financial assistance from CSIR, New Delhi [Scheme No. 01 (2451)/11/EMR-II] and MPCST, Bhopal [Project No. 5986/CST/R&D/2012] is also thankfully acknowledged.

References

[1] K.D. Karlin, Z. Tyeklar. *Bioinorganic Chemistry of Copper*, Chapman and Hall, New York (1993).
[2] B. Reinhammer, *Copper Proteins and Copper Enzymes*, Vol. 3, p. 1, CRC Press, Boca Raton, FL (1984).
[3] K.A. Magnus, H. Ton-That, J.E. Carpenter. *Chem. Rev.*, **94**, 727 (1994).
[4] E.I. Solomon, U.M. Sundaram, T.E. Mackonkin. *Chem. Rev.*, **96**, 2563 (1996).
[5] N. Kitajima, Y. Moro-oka. *Chem. Rev.*, **94**, 737 (1994).
[6] S. Ryan, H. Adams, D.E. Fenton, M. Becker, S. Schindler. *Inorg. Chem.*, **37**, 2134 (1998).
[7] P.L. Holland, W.B. Tolman. *Coord. Chem. Rev.*, **190**, 55 (1999).
[8] H. Decker, R. Dillinger, F. Tuczek. *Angew. Chem. Int. Ed.*, **39**, 1591 (2000).
[9] C. Gerdemann, C. Eicken, B. Krebs. *Acc. Chem. Res.*, **35**, 83 (2002).
[10] G. Dutta, R.K. Debnath, A. Kalita, P. Kumar, M. Sarma, R. Boomi. Shankar, B. Mondal. Polyhedron, **30**, 293 (2011).
[11] M. Valko, M. Mazur, H. Morris, R. Klement, C.J. Williams, M. Melnık. *J. Coord. Chem.*, **52**, 129 (2000).
[12] M. Valko, M. Melnik, H. Morris, R.F. Bilton, P. Pelikan. *Chem. Phys. Lett.*, **183**, 372 (1991).
[13] Y. Muto, H. Horie, T. Tokii, M. Nakashima, M. Koikawa, O.W. Steward, S. Ohba, H. Uekusa, S. Husebye, I. Suzuki, M. Kato. *Bull. Chem. Soc. Jpn.*, **70**, 1573 (1997).

[14] Y. Muto, M. Nakashima, T. Tokii, I. Suzuki, S. Ohba, O.W. Steward, M. Kato. *Bull. Chem. Soc. Jpn.*, **75**, 511 (2002).
[15] J.E. Weder, C.T. Dillon, T.W. Hambley, B.J. Kennedy, P.A. Lay, J.R. Biffin, H.L. Regtop, N.M. Davies. *Coord. Chem. Rev.*, **232**, 95 (2002).
[16] W. Kaim, J. Rall. *Angew. Chem. Int. Ed.*, **35**, 43 (1996).
[17] U. Deuschle, U. Weser. *Prog. Clin. Biochem. Med.*, **2**, 97 (1985).
[18] J.R.J. Sorenson. *Prog. Med. Chem.*, **26**, 437 (1989).
[19] J. Sýkora, J. Sokolík, J. Svec, P. Krätsmár. *Farm. Obzor*, **62**, 349 (1993).
[20] Y.M. Li, C.Y. Xiao, H.R. Feng, S.S. Guo, S.B. Wang. *J. Coord. Chem.*, **65**, 2820 (2012).
[21] W. Xu, H.L. Zhu, J.L. Lin, Y.Q. Zheng. *J. Coord. Chem.*, **66**, 171 (2013).
[22] P.M. Selvakumar, E. Suresh, S. Waghmode, P.S. Subramanian. *J. Coord. Chem.*, **64**, 3495 (2011).
[23] Y. Pang, D. Tian, Y. Luo, X. Zhu, H. Zhang. *J. Coord. Chem.*, **64**, 2002 (2011).
[24] R.N. Patel, S.P. Rawat, M.K. Choudhary, V.P. Sondhiya, D.K. Patel, K.K. Shukla, D.K. Patel, Y. Singh, R. Pandey. *Inorg. Chim. Acta*, **392**, 283 (2012).
[25] G. Giugliarelli, S. Cannistraro, *Nuovo Cimento, 4D Chem.*, **47A**, 353 (2008).
[26] R.N. Patel, K.K. Shukla, A. Singh, M. Choudhary, U.K. Chouhan, S. Dwivedi. *Inorg. Chim. Acta*, **362**, 4891 (2009).
[27] R.N. Patel, K.K. Shukla, A. Singh, K.K. Shukla, D.K. Patel, V.P. Sondhiya, S. Dwivedi. *J. Sulfur Chem.*, **31**, 299 (2010).
[28] R.N. Patel, D.K. Patel, V.P. Sondhiya, K.K. Shukla, Y. Singh, A. Kumar. *Inorg. Chim. Acta*, **405**, 209 (2013).
[29] A. Altomare, G. Cascarno, C. Giacovazzo, A. Gualardi. *J. Appl. Cryst.*, **26**, 343 (2012).
[30] G.M. Sheldrick. *Acta Cryst.*, **64A**, 112 (2008).
[31] L.J. Farrugia. *J. Appl. Crystallogr.*, **30**, 565 (1797).
[32] A.L. Spek. *PLATON, A Multipurpose Crystallographic Tool, Utrecht University*, Utrecht, The Netherlands (2003).
[33] C.F. Macrae, P.R. Edgington, P. McCabe, E. Pidcock, G.P. Shields, R. Taylor, M. Towler, J. van de Streek. *J. Appl. Crystallogr.*, **39**, 453 (2006).
[34] K. Hylond, I. Voisin, H. Bamoun, C. Auclair. *Anal. Biochem.*, **135**, 280 (1983).
[35] R.G. Bhirud, T.S. Shrivastava. *Inorg. Chim. Acta*, **173**, 121 (1990).
[36] A.W. Addison, T.N. Rao, J. Reedijk, G.C. Vershoor. *J. Chem. Soc., Dalton Trans.*, 1349 (1984).
[37] H.J. Schugal. In *Copper Coordination Chemistry, Biochemical and Inorganic Perspectives*, K.D. Karlin, J. Zubieta (Eds.), Adenine Press, New York (1983).
[38] P. Bindu, M.R.P. Kurup, T.R. Satyakeerthy. *Polyhedron*, **18**, 321 (1999).
[39] M. Gaye, S. Sarr, A.S. Sall, O. Diouf, S. Hadabere. *Bull. Chem. Soc. Ethiop.*, **11**, 111 (1997).
[40] B.J. Hathaway, A.E. Underhill. *J. Chem. Soc.*, 3091, (1961).
[41] A.D. Kulkarni, S.A. Patil, P.S. Badami. *J. Sulfur Chem.*, **30**, 145 (2009).
[42] V. Rabjendran, R. Viswanathan, M. Palaniandavar, M. Lakshminarayanan. *J. Chem. Soc., Dalton Trans.*, 3563 (1992).
[43] C. Bathe, C. Beguin, I.G. Luneau, S. Hamman, C. Philouze, J.L. Pierre, F. Thomas, S. Terreli. *Inorg. Chem.*, **41**, 79 (2002).
[44] R.N. Patel. *Inorg. Chim. Acta*, **363**, 838 (2010).
[45] R.R. Gagne, C.A. Koval, T.J. Smith, M.C. Cimlino. *J. Am. Chem. Soc.*, **101**, 4571 (1979).
[46] W.H. Morrison, S. Krogsrud, D.N. Hendrickson. *Inorg. Chem.*, **12**, 1998 (1973).
[47] H. Ohtsu, Y. Schimizaki, A. Odani, O. Yamauchi, W. Mori, S. Itoh, S. Fukuzumi. *J. Am. Chem. Soc.*, **122**, 5733 (2000).
[48] J.A. Moreland, R.J. Doedens. *J. Am. Chem. Soc.*, **97**, 508 (1975).
[49] S. Thakurta, P. Roy, G. Rosair, C.J.G. Garcia, E. Garribba, S. Mitra. *Polyhedron*, **28**, 695 (2009).
[50] A.H. Maki, B.R. McGarvey. *J. Chem. Phys.*, **29**, 31 (1958).
[51] R.G. Bhirud, T.S. Shrivastava. *J. Inorg. Biochem.*, **40**, 331 (1990).
[52] R.N. Patel, S. Kumar, K.B. Pandeya. *J. Inorg. Biochem.*, **89**, 61 (2002).
[53] R.P. Bonomo, E. Conte, G. Irapellizzeri, G. Papalanto, R. Purrello, E. Rizzarelli. *J. Chem. Soc., Dalton Trans.*, 6 (1996).
[54] H. Ohtsu, Y. Shimazaki, A. Odani, O. Yamauchi. *Chem. Commun.*, **2393**, (1999).
[55] W. Kaim, B. Schwederski (Eds.), *Bioinorganic Chemistry: Inorganic Elements in the Chemistry of Life*, Wiley Chichester, p. 209 (1994).